Electronic Materials Letters, Vol. 3, No. 2 (2007), pp. 57-62

Effect of Heavy Arsenic Doping on the *In-situ* Growth of Epitaxial $CoSi_2$ on (100) Si Using Reactive Chemical Vapor Deposition

Heui Seung Lee[1] and Byung Tae Ahn*

Department of Materials Science and Engineering, Korea Advanced Institute of Science and Technology, 373-1 Guseong-dong, Yuseong-gu, Daejeon 305-701, Korea
[1]MagnaChip Semiconductor, Cheongju, Korea

A $CoSi_2$ layer was grown *in-situ* on heavily arsenic-doped Si by reactive chemical vapor deposition of a $Co(\eta^5\text{-}C_5H_5)(CO)_2$ precursor at 650°C. The nucleation and growth mechanism were investigated in comparison with those on undoped Si. In the initial deposition stage, discrete $CoSi_2$ plates with a large area of the {111} coherent planes were nucleated with a deeper penetration depth and a higher density of twinned structure compared to the plates on undoped Si. A thicker $CoSi_2$ layer is necessary for an epitaxial layer with uniform thickness on the heavily arsenic-doped Si. Analyses of the X-ray rocking curve and residual stress indicated that the high As concentration in $CoSi_2$ reduced the lattice mismatch between Si and $CoSi_2$ and reduced the lattice strain.

Key words : $CoSi_2$ silicide, epitaxial growth, carbon mediated growth, *in-situ* growth

1. INTRODUCTION

The self-aligned silicide (salicide) process has been used for gate, source, and drain contact metallization in microelectronics devices. Among leading silicides, $CoSi_2$ is the most promising due to its low resistivity and line-width-independent sheet resistance. Epitaxial $CoSi_2$ layers, as opposed to polycrystalline $CoSi_2$ layers, are of special interest due to their enhanced thermal stability and shallow junction formation using a silicide-as-doping-source (SADS) process. Due to the small lattice mismatch (-1.2%) with respect to Si and due to its similar crystal structure (CaF_2 structure), $CoSi_2$ can be epitaxially grown on Si substrates. Several growth techniques including titanium interlayer-mediated epitaxy, oxide-mediated epitaxy, CoC_x-mediated epitaxy have been introduced to produce the $CoSi_2$/Si heteroepitaxy structure[1-3]. In addition, a uniform epitaxial $CoSi_2$ layer of good quality can be grown *in-situ* on a (100) Si substrate heated above 600°C by controlling the Co flux in a simple metal-organic chemical vapor deposition (MOCVD) reactor[4]. In this case, a very thin carbon interlayer acts as an interlayer that suppresses the supply of Co from the gas phase. Recently, it was found that an in-situ grown $CoSi_2$ layer is thermally stable at much higher temperatures than a layer formed by a conventional Co/Si solid-state reaction[5,6].

In the salicide process, silicides are grown on heavily doped source/drain regions and polycrystalline silicon gates. Little data is available on the effect of dopants during the growth of $CoSi_2$. *In-situ* monitoring of the emissivity during the Co/Si reaction on heavily arsenic-doped Si has indicated that arsenic retards the nucleation of polycrystalline $CoSi_2$[7]. No report has been published regarding the effect of the arsenic dopant on the epitaxial growth of $CoSi_2$. In the present study, the growth behavior of epitaxial $CoSi_2$ layers on heavily arsenic-doped Si by reactive chemical-vapor deposition was investigated in relation to undoped Si.

2. EXPERIMENTAL

P-type (100) Si wafers with a resistivity of 5-8 Ω· cm and heavily arsenic-doped (100) Si wafers were used as substrates. Arsenic was implanted at a dose of 6×10^{15}/cm^2 at 40 keV with a 10 nm thick screen oxide. Following ion implantation, furnace annealing was carried out at 900 °C for 20 min in N_2 to activate arsenic and recover implant damage. The Si wafers were cleaned in a H_2SO_4/H_2O_2 solution, rinsed in de-ionized water, dipped in HF(1%), rinsed again in de-ionized water, and then loaded into an MOCVD reactor. The Co was supplied to the Si substrate heated to 650°C using cyclopentadienyl dicarbonyl cobalt, $Co(\eta^5\text{-}C_5H_5)(CO)_2$, at 100 mTorr with 10 sccm H_2 carrier gas. The temperature of a bubbler was held at -3°C to reduce the vapor pressure.

The crystal structure and microstructure of the samples were investigated using X-ray diffraction (XRD) and transmission electron microscopy (TEM), respectively. The

*Corresponding author: btahn@ kaist.ac.kr

arsenic dopant distribution was investigated using secondary-ion mass spectrometry (SIMS). The lattice parameter of the $CoSi_2$ layer was analyzed by an X-ray rocking curve using high-resolution X-ray diffraction (HRXRD). The residual stress of the as-deposited film on Si was examined by measuring the radius of curvature using a stress gauge (Tencor FLX-2320).

3. RESULTS AND DISCUSSIONS

Figure 1 shows the XRD patterns of the samples as-deposited at 650°C for 15 min from the $Co(\eta^5\text{-}C_5H_5)(CO)_2$ precursor on (a) undoped Si and (b) heavily arsenic-doped Si. Only $CoSi_2$ (200) and Si (200) peaks exist. Other peaks such as $CoSi_2$ (111) and (220) were not found. It is seen that a $CoSi_2$ layer with strong (100) preferred-orientation was grown by the reaction between Co and Si on both substrates. The peak intensity of $CoSi_2$ (200) on heavily As-doped Si is weaker than that on undoped Si.

The formation of $CoSi_2$ plates in the initial deposition stage was investigated using a TEM plan-view and a cross-sectional view. Figure 2 shows plan-view bright-field TEM

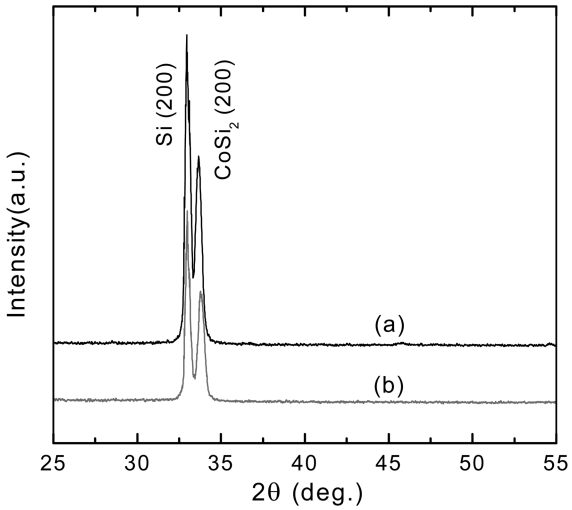

Fig. 1. XRD patterns of samples deposited at 650°C for 15 min from $Co(\eta^5\text{-}C_5H_5)(CO)_2$ on (a) heavily As-doped Si and (b) undoped Si.

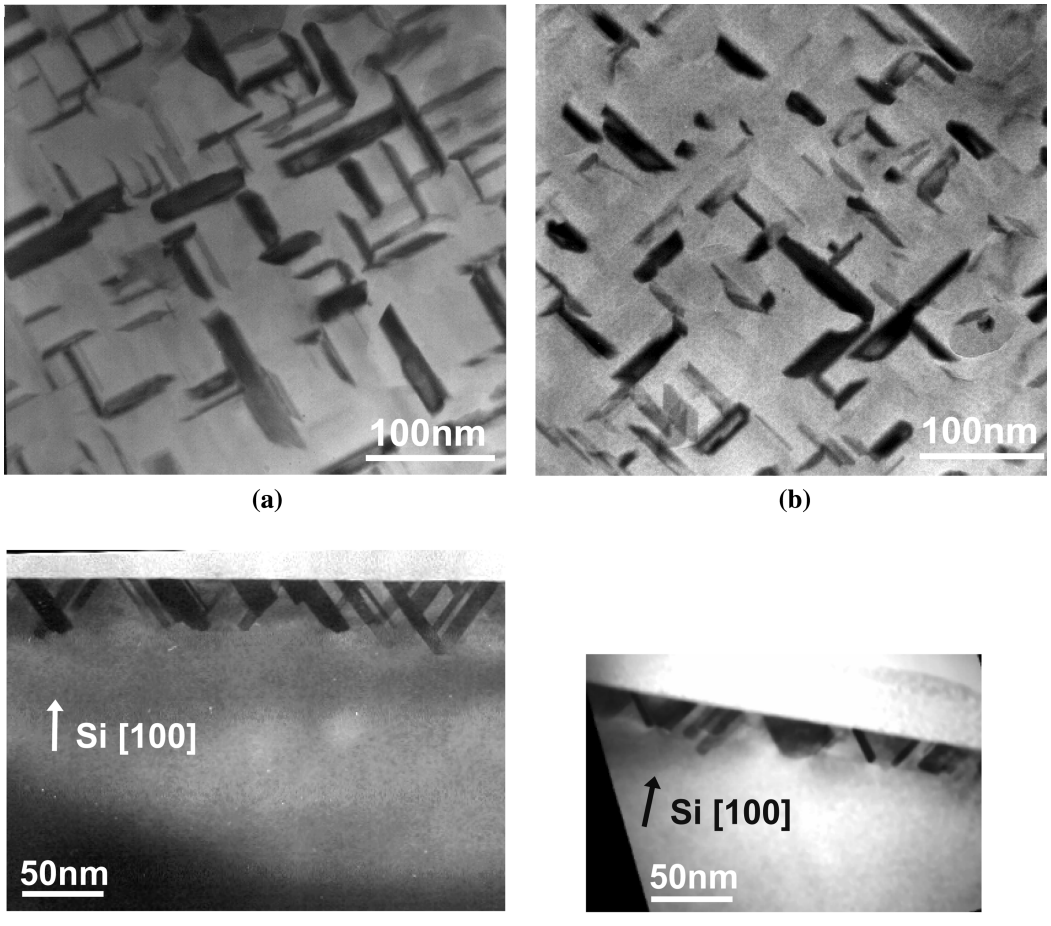

Fig. 2. Plan-view bright-field TEM micrographs and cross-sectional TEM micrographs of samples deposited at 650°C for 5 min on (a, c) heavily As-doped Si and (b, d) undoped Si.

micrographs as well as cross-sectional TEM micrographs of the samples deposited at 650°C for 5 min on (a, c) heavily As-doped Si and (b, d) undoped Si. In Figs. 2a and 2b, two-dimensionally elongated $CoSi_2$ islands are formed and aligned along the <011> directions on a (100) Si plane. The $CoSi_2$ nuclei grew as long rods with two different orientations. At the initial deposition stage, the sizes of the $CoSi_2$ plates on the heavily As-doped Si were observed to be larger than those on undoped Si. The density of the $CoSi_2$ nuclei on the heavily As-doped Si is similar to that on the undoped Si. In Figs. 2c and 2d, the $CoSi_2$ plates grew along the <112> directions with large {111} interfaces. The maximum depths of the $CoSi_2$ plates along the [100] direction on heavily As-doped Si and undoped Si are approximately 46 nm and about 25 nm, respectively. Plate-shaped $CoSi_2$ nuclei appear when grown by carbon-mediated growth, while a continuous layer of $CoSi_2$ nuclei appears when grown by CoN_x-mediated growth[8,9].

Figure 3 shows (a) the selected-area-diffraction-pattern (SADP) and (b) its schematic representation for a sample deposited at 650°C for 5 min on heavily As-doped Si along the [011] zone axis. The SADP shows an orientation relationship of $CoSi_2[011] \parallel Si[011]$, excluding the extra spots that exist at the 1/3 position from the main diffracted Si spots. The extra spots are thought to originate from the twinned structure (type-B) of the $CoSi_2$ plates. Type-B $CoSi_2$ is rotated 180° about the surface normal <111> axis compared to $CoSi_2$ with the same orientation as the Si substrate (type-A)[10,11].

Figure 4 shows plan-view dark-field TEM micrographs obtained with the $CoSi_2$ (002) diffraction spot and their SADPs along the [100] zone axis of the samples grown at 650°C with 5 min of deposition on (a) heavily As-doped Si and (b) undoped Si. The diffraction spots from $CoSi_2$ and Si in the SADP nearly coincide with each other, with the exception of the $CoSi_2$ {002} spot. In the dark-field image obtained with the $CoSi_2$ (002) diffraction spot along the [100] zone axis, only the type-A $CoSi_2$ appears bright, whereas the type-B $CoSi_2$ does not. From a comparison of the dark-field images, the density of the type-A $CoSi_2$ on the heavily As-doped Si was found to be smaller than that on

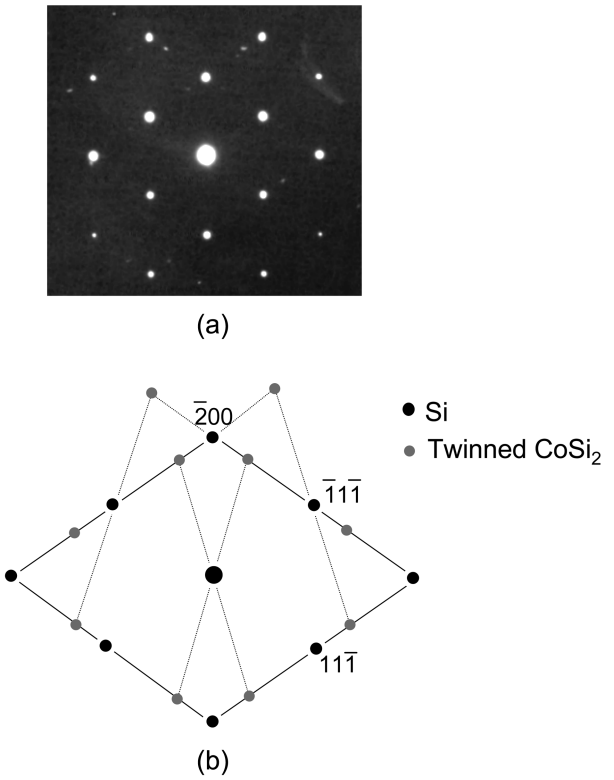

Fig. 3. (a) Selected-area-diffraction-pattern and (b) its schematic representation for a sample deposited at 650°C for 5 min on heavily As-doped Si along the [011] zone axis.

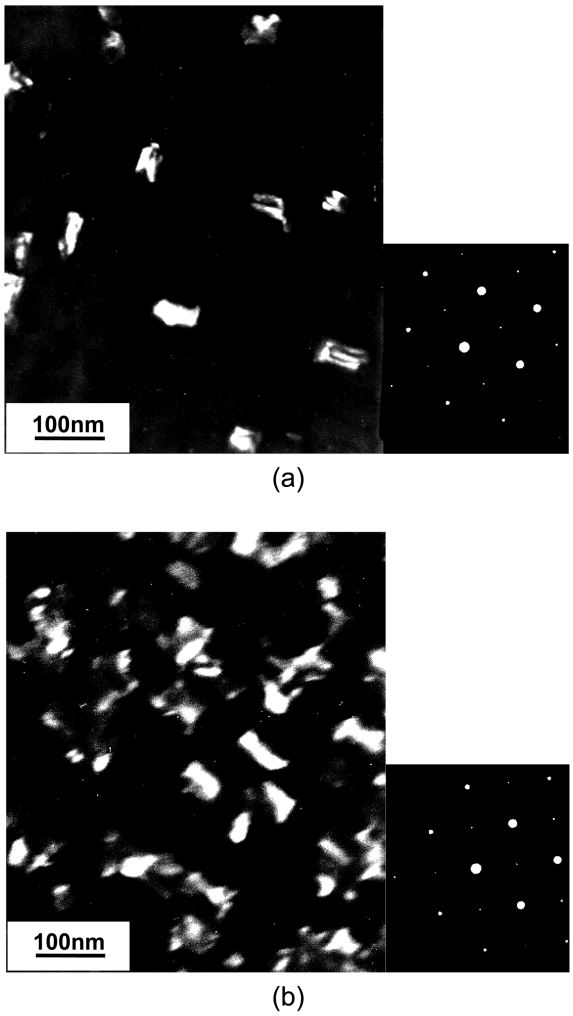

Fig. 4. Plan-view dark-field TEM images obtained with $CoSi_2$ (002) diffraction spot and their SADPs along the [100] zone axis of the samples grown at 650°C for 5 min deposition on (a) heavily As-doped Si and (b) undoped Si.

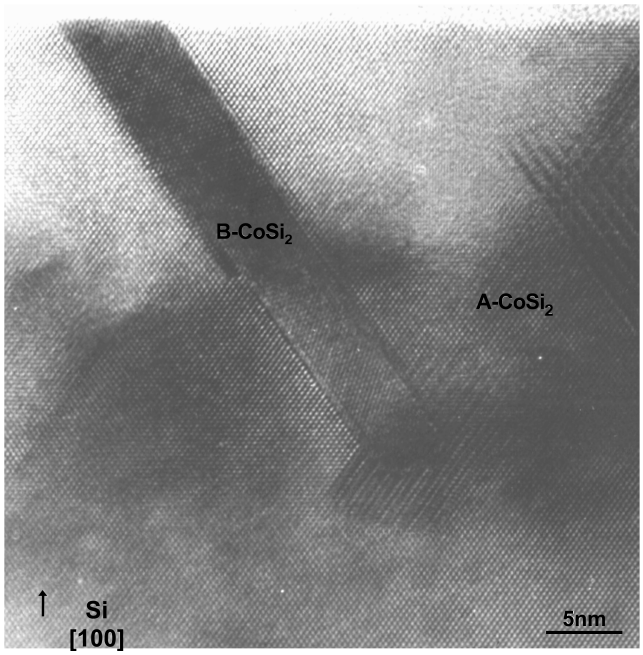

Fig. 5. HRTEM micrograph along the [011] zone axis of a sample deposited at 650°C for 5 min on heavily As-doped Si.

undoped Si. As the densities of the $CoSi_2$ nuclei on the heavily As-doped Si and undoped Si are similar, it can be said that the type-B $CoSi_2$ plates are dominantly nucleated on the heavily As-doped Si.

A high-resolution TEM (HRTEM) image along the [011] zone axis was taken to investigate the coherency at the interface of $CoSi_2$/Si of the as-deposited sample at 650°C with 5 min of deposition on the heavily As-doped Si. The lattice image in the HRTEM image shown in Fig. 5 shows that the $CoSi_2$ plate has coherent {111} interfaces. Both type-A $CoSi_2$ and type-B $CoSi_2$ are shown in the HRTEM image. Moiré fringes, originating from the lattice rotation often observed in epitaxial growth, were also found in the overlapped region of the $CoiSi_2$ nuclei.

Figure 6 shows cross-sectional TEM micrographs of samples deposited at 650°C for (a) 15 min, and (b) 25 min on heavily As-doped Si, and for (c) 15 min on undoped Si. After deposition for 15 min, the $CoSi_2$ layers are continuous on both substrates. After deposition for 25 min on heavily As-doped Si, a $CoSi_2$ layer approximately 46-nm thick was grown with a large flat (100) interface with a protrusion approximately 75-nm thick. On the heavily As-doped Si, the formation of a uniform $CoSi_2$ layer required a larger $CoSi_2$ thickness. In addition, deeper protrusions exist during the formation of a uniform layer.

The diffraction spots from $CoSi_2$ and Si in the SADP at the $CoSi_2$/Si interface for the sample deposited for 25 min on heavily As-doped Si nearly coincide with each other, apart from the extra spots, indicating that the $CoSi_2$ layer was epitaxially grown on heavily As-doped Si. On the undoped Si, the type-B $CoSi_2$ disappears and only the type-A $CoSi_2$ exists[4]. However, the type-B $CoSi_2$ still exists on heavily As-doped Si, as shown in the SADP in Fig. 6b.

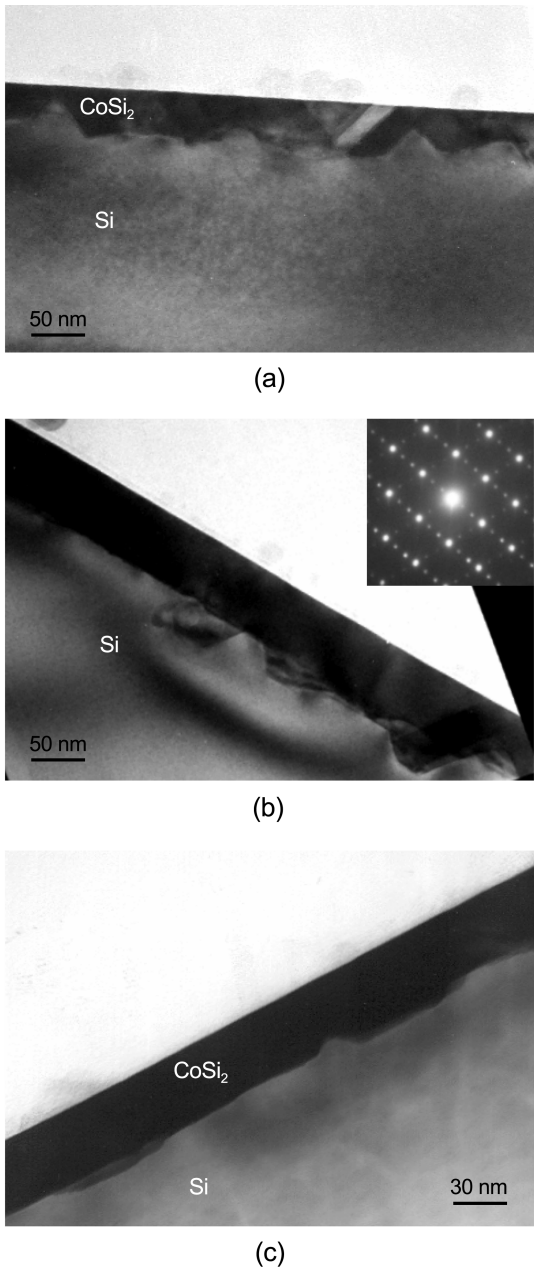

Fig. 6. Cross-sectional TEM micrographs of samples deposited at 650°C for (a) 15, (b) 25 min on heavily As-doped Si and (c) 15min on undoped Si.

Figure 7 shows the SIMS As profile for a sample with a $CoSi_2$ layer grown at 650°C for 25 min on heavily As-doped Si. The As concentration at the $CoSi_2$/Si interface is nearly $1.1 \times 10^{21}/cm^3$, which is higher than the original As concentration ($8.0 \times 10^{20}/cm^3$) in Si, indicating that a pile-up of As atoms in the region near the $CoSi_2$/Si interface occurs. Man-

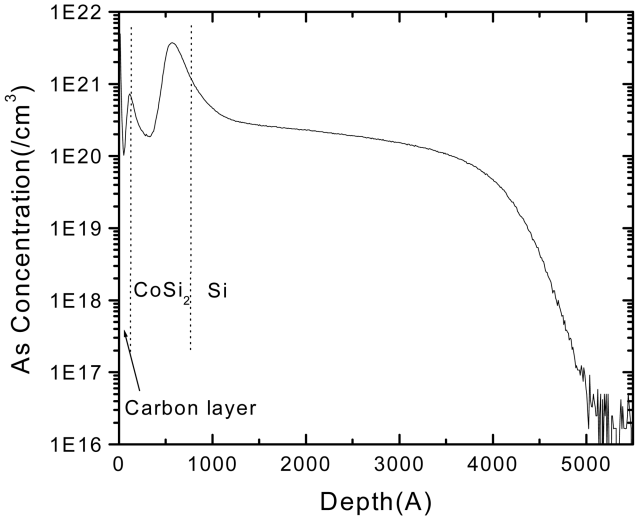

Fig. 7. SIMS depth profile of As for sample with $CoSi_2$ layer grown at 650°C for 25 min on heavily As-doped Si.

gelinck et al. reported that the solid solubility of As in a $CoSi_2$ is lower than that in Si[12]. The As atoms are pushed away from $CoSi_2$ into the Si region during the growth of $CoSi_2$ due to the difference in the solid solubility. The diffusivities of the As atoms in $CoSi_2$ and Si at 650°C are 7.1×10^{-18} and 9.4×10^{-22} cm^2/s, respectively[12,13]. As the diffusivities are too small to be at equilibrium in Si, the As concentration near the $CoSi_2$/Si interface increases. The high As concentration in $CoSi_2$ near the interface may cause a more significant increase of $CoSi_2$ lattice parameters compared to Si, as the lattice parameters of $CoSi_2$ are smaller than Si.

Figure 8 shows the X-ray rocking curves for the samples deposited at 650°C for (a) 5 and (b) 15 min on heavily As-doped Si and undoped Si. In Fig. 8a, a weak $CoSi_2$ (400) peak to the right of the Si (400) peak appears broadly on undoped Si after deposition at 650°C for 5 min. However, a $CoSi_2$ (400) peak rarely exists on heavily As-doped Si. Type-B $CoSi_2$ does not have a $CoSi_2$ (400) plane parallel with the (400) plane of the (100) Si substrate. Therefore, from a comparison of the $CoSi_2$ (400) peak intensities of the X-ray rocking curves, said it is clear that the density of the type-B $CoSi_2$ plates on heavily As-doped Si is much higher than that on undoped Si. This result is in good agreement with the result of the dark-field TEM micrograph shown in Fig. 4.

In Fig. 8b, a $CoSi_2$ (400) peak of a sample grown at 650°C for 15 min on heavily As-doped Si appears farther away from the Si (400) peak than that of the sample grown on undoped Si. This indicates that the lattice parameter of $CoSi_2$ along the [100] direction becomes smaller on heavily As-doped Si. If a partially strain-relaxed layer is assumed[14], the lattice constants of $CoSi_2$ on the (100) plane increase as the lattice constant of $CoSi_2$ decreases along the [100] direction. It appears that the lattice constants of $CoSi_2$ on the (100) plane increase more significantly with the high concentration of As in $CoSi_2$. However, the lattice constant of Si rarely changes with the high concentration of As in the Si, as seen in the Si (400) peaks. Therefore, the lattice parameters of $CoSi_2$ on the (100) plane are larger on heavily As-doped Si, and the in-plane lattice mismatch on heavily As-doped Si is smaller than on undoped Si.

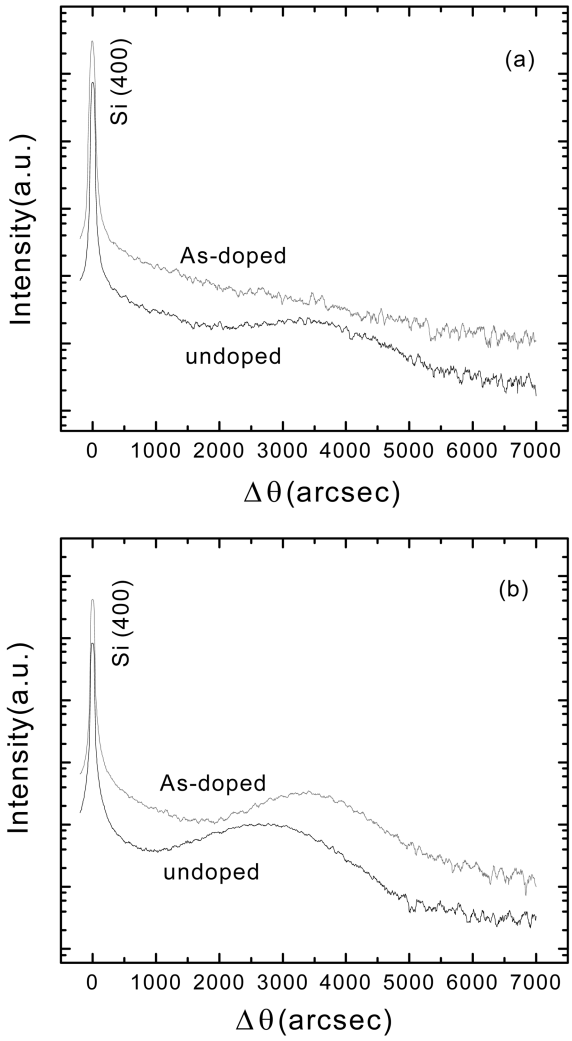

Fig. 8. X-ray rocking curves for samples deposited at 650°C for (a) 5 and (b) 15 min on heavily As-doped Si and undoped Si.

The residual stress of the films was examined by measuring the radius of curvature using Stoney's equation:[15]

$$\sigma = [E/(1-\nu)]_{Si} \cdot t_s^2 / 6\, t_f\, (R^{-1} - R_o^{-1}).$$

Here, σ is the stress, E is the Young's modulus, ν is Poisson's ratio, t_s is the thickness of the substrate, and t_f is the thickness of the film. R and R_0 are the radii of the curvature of the substrate after and before film formation, respectively. Due to the large difference in the thermal-expansion coefficients of $CoSi_2$ (9.4×10^{-6} K^{-1}) and Si (2.3×10^{-6} K^{-1}) and the

Table 1. Residual stress of the $CoSi_2$ layers grown on heavily As-doped Si and undoped Si (unit: MPa)

Substrate Deposition condition	heavily As-doped Si	undoped Si
650°C, 7 min	376 (compressive)	742 (tensile)
650°C, 15 min	1891 (tensile)	963 (tensile)

difference in the volume of $CoSi_2$ and Si, residual stress in the $CoSi_2$ layer usually becomes tensile at room temperature[16].

Table 1 shows the residual stress of the $CoSi_2$ layers grown on heavily As-doped Si and undoped Si. After deposition at 650°C for 15min, the residual stress of the $CoSi_2$ layer is tensile on both substrates. The stress value on heavily As-doped Si is approximately 1.89 GPa, which is higher than that on undoped Si. To investigate the effect of stress on the $CoSi_2$ nuclei in the initial deposition stage, the residual stress was measured after deposition at 650°C for 7 min. The $CoSi_2$ plates were found to be discrete after deposition for 7 min. Although the $CoSi_2$ plates are not continuous, the $CoSi_2$ and Si matrix are assumed to be a layer, and the thickness is the maximum growth depth of the $CoSi_2$ plate from the TEM micrograph. As the stress value in the initial deposition stage was calculated using this assumption, the absolute value of the stress could not be correct but the tendency could be correct. The residual stress of the ($CoSi_2$ + Si)-mixed layer of the sample deposited at 650°C for 7 min for heavily As-doped Si was compressive, while that for undoped Si was tensile. In the initial deposition stage, compressive stress on heavily As-doped Si can result from an increase in the average volume of $CoSi_2$ molecules with existence of As atoms in the $CoSi_2$ layer. The volume increase of $CoSi_2$ molecules can reduce the lattice mismatch between $CoSi_2$ and Si, causing a reduction of $CoSi_2$/Si interfacial energy and a reduction of strain energy. The reductions in the interfacial energy and strain energy can result in an increase in the penetration depth of $CoSi_2$ plates along the <112> direction on heavily As-doped Si, as shown in Fig. 2.

4. CONCLUSIONS

The nucleation and growth mechanism of an epitaxial $CoSi_2$ layer grown *in-situ* on heavily As-doped Si by reactive chemical-vapor deposition of $Co(\eta^5\text{-}C_5H_5)(CO)_2$ was investigated. In the initial deposition stage, discrete $CoSi_2$ plates on heavily As-doped Si were nucleated with a deeper penetration depth. In addition, they had a higher density of type-B $CoSi_2$, compared to plates on undoped Si. A thicker $CoSi_2$ layer is necessary for an epitaxial layer with uniform thickness on heavily As-doped Si. From analyses of the X-ray rocking curve and residual stress, it was shown that As atoms in the $CoSi_2$ reduced the lattice mismatch and the lattice strain between Si and $CoSi_2$.

ACKNOWLEDGMENT

This work was financially supported by the Korea Research Foundation through the Center for Nano Interface Research (KRF-2005-005-J09702).

REFERENCES

1. M. L. A. Dass, D. B. Fraser, and C. S. Wei, *Appl. Phys. Lett.* **58**, 1308 (1991).
2. R. T. Tung, *Appl. Phys. Lett*. **68**, 3461 (1996).
3. H. S. Rhee, T. W. Jang, and B. T. Ahn, *Appl. Phys. Lett.* **74**, 1003 (1999).
4. H. S. Rhee and B. T. Ahn, *Appl. Phys. Lett.* **74**, 3176 (1999).
5. H. S. Lee, H. S. Rhee, and B. T. Ahn, *J. Electrochem. Soc.* **149**, G16 (2002).
6. J. E. Hong, S. I. Kim, H. S. Lee, and B. T. Ahn, *Jap. J. Appl. Physics* **45**, 710 (2006).
7. R. J. Schreutelkamp, P. Vandenaheele, B. Deweerdt, W. Coppye, C. Vermeiren, A. Lauwers, and K. Maex, *Appl. Phys. Lett*. **61**, 2296 (1992).
8. S. I. Kim, S. R. Lee, J. H. Park, and B. T. Ahn, *J. Electrochem. Soc.* **153**, G506 (2006).
9. S. I. Kim, S. R. Lee, J. H. Park, and B. T. Ahn, *Electrochem. Solid-State Lett.* **8**, G324 (2005).
10. R. T. Tung and J. L. Batstone, *Appl. Phys. Lett.* **52**, 1611 (1988).
11. S. Mantl, *J. Phys. D: Appl. Phys*. **31**, 1 (1998).
12. D. Mangelinck, J. Cardenas, F. M. d'Heurle, B. G. Svensson, and P. Gas, *J. Appl. Phys.* **86**, 4908 (1999).
13. W. E. Beadle, J. C. C. Tsai, and R. D. Plummer, *Quick Reference Manual for Silicon Integrated Circuit Technology*, pp. 6-29, John Wiley & Sons (1985).
14. C. R. Wie, *Mater. Sci. Eng.* **R.13**, 1 (1994).
15. G. G. Stoney, *Proc. R. Soc. London, Ser.* **A82**, 172 (1909).
16. A. H. van Ommen, C. W. T. Bulle-Lieuwma, and C. Langereis, *J. Appl. Phys.* **64**, 2706 (1988).